doi: 10.3389/fnana.2011.00064

Alterations in apical dendrite bundling in the somatosensory cortex of 5-HT_{3A} receptor knockout mice

Laura A. Smit-Rigter, Wytse J. Wadman and Johannes A. van Hooft*

Swammerdam Institute for Life Sciences, Center for Neuroscience, University of Amsterdam, Amsterdam, Netherlands

Edited by:
Javier DeFelipe, Cajal Institute, Spain

Reviewed by:
Kathleen S. Rockland, Massachusetts Institute of Technology, USA
Alfonso Fairén, University Miguel Hernandez, Spain

****Correspondence:***
Johannes A. van Hooft, Swammerdam Institute for Life Sciences, Center for Neuroscience, University of Amsterdam, P.O. Box 94232, 1090 GE Amsterdam, Netherlands.
e-mail: j.a.vanhooft@uva.nl

In various species and areas of the cerebral cortex, apical dendrites of pyramidal neurons form clusters which extend through several layers of the cortex also known as dendritic bundles. Previously, it has been shown that 5-HT_{3A} receptor knockout mice show hypercomplex apical dendrites of cortical layer 2/3 pyramidal neurons, together with a reduction in reelin levels, a glycoprotein involved in cortical development. Other studies showed that in the mouse presubicular cortex, reelin is involved in the formation of modular structures. Here, we compare apical dendrite bundling in the somatosensory cortex of wildtype and 5-HT_{3A} receptor knockout mice. Using a microtubule associated protein-2 immunostaining to visualize apical dendrites of pyramidal neurons, we compared dendritic bundle properties of wildtype and 5-HT_{3A} receptor knockout mice in tangential sections of the somatosensory cortex. A Voronoi tessellation was performed on immunostained tangential sections to determine the spatial organization of dendrites and to define dendritic bundles. In 5-HT_{3A} receptor knockout mice, dendritic bundle surface was larger compared to wildtype mice, while the number and distribution of reelin-secreting Cajal–Retzius cells was similar for both groups. Together with previously observed differences in dendritic complexity of cortical layer 2/3 pyramidal neurons and cortical reelin levels, these results suggest an important role for the 5-HT_3 receptor in determining the spatial organization of cortical connectivity in the mouse somatosensory cortex.

Keywords: column, neocortex, development, serotonin, Cajal–Retzius, reelin

INTRODUCTION

In various species and areas of the cerebral cortex, ascending apical dendrites of pyramidal neurons are organized in clusters also referred to as dendritic bundles (Fleischhauer et al., 1972; Peters and Walsh, 1972; Escobar et al., 1986; Peters and Kara, 1987; White and Peters, 1993; Lev and White, 1997; Ichinohe et al., 2003a; Vercelli et al., 2004). Also in the mouse somatosensory cortex, dendritic bundles of ascending apical dendrites of pyramidal neurons have been observed through several layers of the cortex and their properties described (Escobar et al., 1986; White and Peters, 1993). These dendritic bundles could form the basis of small functional units of vertically interconnected pyramidal and non-pyramidal neurons called cortical modules, yet so far functional evidence is lacking for this hypothesis (Peters and Sethares, 1996; Lev and White, 1997; Rockland and Ichinohe, 2004).

Recently, our group found that Cajal–Retzius cells, a population of cells which play an important role in cortical development by secreting the glycoprotein reelin (D'Arcangelo et al., 1995), express the 5-HT_3 receptor and that serotonin is the main excitatory drive for these cells (Chameau et al., 2009). Moreover, we showed that in the postnatal cortex, the serotonin 5-HT_3 receptor plays a pivotal role in the regulation of apical dendrite arborization of cortical layer 2/3 pyramidal neurons via a reelin-dependent pathway (Chameau et al., 2009). In mice lacking the 5-HT_{3A} receptor, we found a reduction in reelin levels and a hypercomplex dendritic tree of apical dendrites of layer 2/3 pyramidal neurons in the somatosensory cortex (Chameau et al., 2009).

To date, a number of factors have been implicated to play a role in dendritic bundle formation such as neurotrophins, cell adhesion molecules, gap junctions, and cytoskeletal changes (Ichinohe et al., 2003b; Miyashita et al., 2010). As will be discussed later, the formation of dendritic bundles in several areas of the cortex most likely results from a complex interplay between these factors. Interestingly, in the mouse presubicular cortex, also reelin is involved in the formation of modular structures (Nishikawa et al., 2002; Janusonis et al., 2004). In neonatal mice of which the serotonergic innervation to Cajal–Retzius cells was disrupted, reelin levels were decreased, and cortical column organization was also disrupted (Janusonis et al., 2004). Given this observation, we hypothesized that together with the alterations in reelin levels and dendritic complexity of cortical pyramidal neurons, mice lacking the 5-HT_{3A} receptor show alterations in the organization of dendritic bundles in the somatosensory cortex.

In the current study, we investigated the organization of dendritic bundles of ascending apical dendrites of pyramidal neurons in the somatosensory cortex of 5-HT_{3A} receptor knockout mice and compared them with wildtype mice. The properties of the dendritic bundles were compared in microtubule associated protein (MAP)-2 immunostained tangential sections from layer 3 of the somatosensory cortex. In addition, we investigated the number and distribution of reelin-secreting Cajal–Retzius cells in both groups.

MATERIALS AND METHODS

ANIMALS

Both male and female C57BL/6J wildtype and 5-HT_{3A} knockout mice (Zeitz et al., 2002) were used. In this study, 5-HT_{3A} knockout mice were maintained on the C57BL/6J background and back-crossed for at least 35 generations. From weaning (postnatal day 21) onward, offspring was group-housed (four per cage), with access to food and water *ad libitum* on a 12/12-h light dark cycle according to the guidelines of the animal welfare committee of the University of Amsterdam.

IMMUNOHISTOCHEMISTRY

At postnatal day (P) 4 and 14 and at 4 months of age, 3–8 mice per group were deeply anesthetized with a lethal i.p. dose of euthasol and perfused with 0.1 M PBS, pH = 7.4, followed by 4% paraformaldehyde in PBS. Brains were dissected and after 1 h of postfixation, hemispheres were separated and one hemisphere was flattened between two plastic foil-covered glass slides. After 24 h of postfixation, both intact and flattened brains were kept in 0.25% paraformaldehyde in PBS. Forty micrometer thick coronal and tangential slices were cut on a vibroslicer (Leica VT1000S) and collected in PBS.

For the MAP-2 immunostaining, both coronal and tangential slices from adult mice were rinsed with PBS and endogenous peroxidases were removed with 3% H_2O_2 in PBS for 30 min, then slices were incubated in 0.1% triton-X and 5% NGS in PBS for 1 h. Subsequently, slices were incubated overnight at 4°C with 1:1500 MAP-2 HM-2 anti-mouse primary antibody (Sigma) in 0.1% triton-X and 5% NGS in PBS. The next day, slices were rinsed with PBS and incubated with 1:200 biotinylated sheep anti-mouse secondary antibody (Amersham) in 0.1% triton-X and 5% NGS in PBS for 1 h, rinsed again with PBS, incubated with ABC (Vector labs UK) for 2 h and visualized with a DAB (Invitrogen USA) reaction. After 3 min, reaction was stopped and slices were mounted with moviol. The next day, images of the somatosensory cortex were captured using a Zeiss FS2 microscope with a 20× objective: dry Plan Neofluor 20×/0.50 and with Image Pro software.

For the reelin staining, tangential slices from P4 and P14 mice were rinsed with PBS and incubated in 0.25% triton-X and 10% NGS in PBS for 1 h. Subsequently, slices were incubated overnight at 4°C with 1:1000 G-10 anti-mouse primary antibody (Abcam) in 0.25% triton-X and 5% NGS in PBS. The next day, slices were rinsed with PBS and incubated with 1:250 Alexa 488-conjugated goat anti-mouse (Molecular Probes) in 0.25% triton-X and 5% NGS in PBS for 2 h. Again, slices were rinsed and mounted on glass slides with Vectashield (Vector labs UK). Images were scanned on a confocal microscope (Zeiss LSM 510). Objective: dry Plan Neofluor 20×/0.75.

DENDRITIC BUNDLE ANALYSIS

Tangential maps of 0.244 mm^2 through layer 3 (between 250 and 350 μm from the pial surface) were taken from sections immunostained for MAP-2. The mean dendrite diameter was determined as a mean of 20 apical dendrites per animal in layer 3 of the primary somatosensory cortex (in all sections barrels were visible in layer 4) and all apical dendrites were located (x–y-coordinates). This analysis was performed using ImageJ software (**Figure 1A**). The location data were further analyzed with custom-made software written in MATLAB (MathWorks version 2007b).

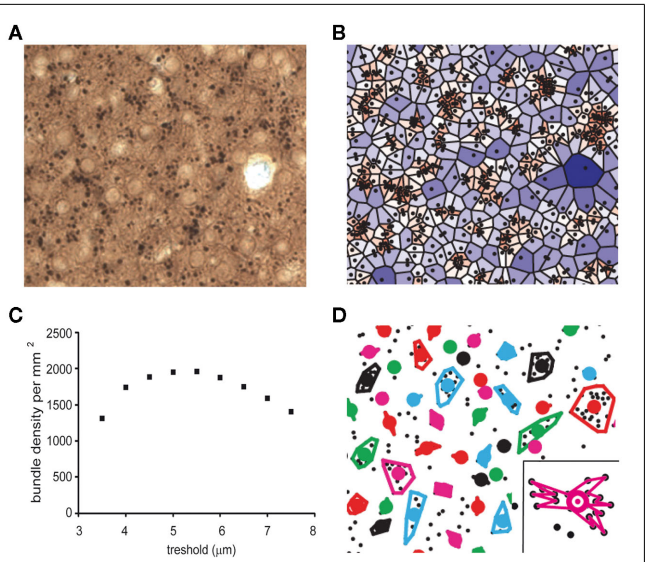

FIGURE 1 | Quantitative analysis of dendritic bundles in the mouse somatosensory cortex. (A) Typical example of a MAP-2 immunostained tangential section showing clusters of ascending apical dendrites of pyramidal neurons (black dots). **(B)** Surface polygons as determined by the Voronoi tessellation (borders excluded), are marked by a color scale that indicates surface. Values range from small (red) to large (blue). **(C)** The mean dendritic bundle density per mm^2 in layer 3 of the somatosensory cortex of wildtype mice remains similar when the nearest neighbor distance threshold varies from 4.5 to 6 μm. **(D)** Using a nearest neighbor distance threshold of 5.5 μm and a minimum of three dendrites per bundle, bundles are now determined and bundle surface can be calculated in two different ways: (1) as the surface of the polygon with the smallest circumference that includes all dendrites (as shown in figure) or (2) as the surface of the polygon that connects all dendrites continuously (see inset). Colored circles represent the location of the bundles (see Materials and Methods).

In order to analyze the spatial distribution pattern of dendrites and in particular to determine if they are clustered in bundles, we defined the "local dendritic density" by uniquely attributing each point in space to the closest dendrite. The mathematical procedure to accomplish this, is called a Voronoi Tessellation and it has been used before on neuronal structures (Duyckaerts and Godefroy, 2000). A Voronoi tessellation or Voronoi diagram partitions a plane with n points into n convex polygons such that each polygon contains exactly one generating point and every point in a given polygon is closer to its generating point than to any other. In the case of our tangential sections of the cortex, "points" are the cross-sectioned apical dendrites (**Figure 1B**) and each dendrite is uniquely linked to a fraction of the total surface, which defines the local dendritic density. The coefficient of variation (CV) for the complete tessellation is given by inverse ratio between the average polygon area and its SD. A (Monte-Carlo style) study by Duyckaerts et al. (1994) demonstrated that the CV value of a polygon surface is indicative for the nature of the spatial organization of the dendrites: a CV value larger than 0.64 implies that the dendrites are clustered while a value less than 0.36 indicates a

regularly distributed spatial organization of the dendrites, for CV equal to 0 the organization is completely regular. CV values that lie between 0.36 and 0.64 represent a randomly distributed spatial organization of the dendrites.

A second application of the Voronoi tessellation is that it links each dendrite to a unique set of neighbors, which implies that we can uniquely define and calculate the inter-neighbor distances. Using a simple threshold criterion in the inter-dendrite distance we can now determine which dendrites belong to the same bundle. If the threshold value is set too small, there will be no bundles and if it is set too high, they will all belong to the same bundle. The relation between threshold (range 3.5–7.5 μm) and calculated bundle density (**Figure 1C**) shows an optimum between 4.5 and 6 μm. This relation was similar for wildtype and 5-HT$_{3A}$ receptor knockout mice and for the rest of the study we choose a fixed threshold of 5.5 μm to define bundles. To prevent that single dendrites or pairs show up as bundles, we also required that a bundle needed to consist of at least three dendrites in order to qualify as such (**Figure 1D**). Around 75% of the dendrites were located in bundles, a substantial number of the excluded dendrites were located at the border of the investigated region.

Once a bundle was defined as consisting of n dendrites, its location (x_b, y_b) was calculated as its center of gravity: $x_b = (\Sigma x_i)/n$ and $y_b = (\Sigma y_i)/n$. Next bundle surface was calculated in two different ways: (1) as the area of the polygon that connects all dendrites continuously (see inset **Figure 1D**) or (2) as the area of the polygon with the smallest circumference that includes all dendrites (see other bundles **Figure 1D**). The first measure was systematically about 0.69 of the second one. We therefore present here only the second measure (see **Figure 5**). With these definitions a set of parameters was calculated that characterizes the bundles and their organization. The spatial aspect of the dendritic bundles was then assessed by a second Voronoi tessellation now performed using the bundle locations (x_b, y_b) as the starting points.

ANALYSIS OF THE DISTRIBUTION OF REELIN-POSITIVE CAJAL–RETZIUS CELLS

In tangential sections of 0.21 mm^2 through layer 1 immunostained for reelin, the location of all reelin-positive Cajal–Retzius cells was determined, comparable to the determination of dendrite location, using ImageJ software. On these coordinates a Voronoi tessellation was performed in order to determine the spatial organization of the Cajal–Retzius cells.

STATISTICAL ANALYSIS

All data are expressed as mean ± SE of the mean (SEM). Unless otherwise mentioned, values were compared with Student's *t*-test. $p < 0.05$ was used to indicate a significant difference (in graphs indicated as *).

RESULTS

In both wildtype and 5-HT$_{3A}$ receptor knockout mice, ascending apical dendrites of pyramidal neurons extend toward the pial surface in MAP-2 immunostained coronal sections of the somatosensory cortex (**Figure 2**). In these coronal sections of the somatosensory cortex, apical dendrites of pyramidal neurons from upper layers adjoin apical dendrites of pyramidal neurons from deeper layers to form clusters also known as dendritic bundles. A repetitive pattern of dendritic bundles of ascending apical dendrites through several layers of the cortex was visible, allowing quantification of the spatial organization of dendrites in MAP-2 immunostained tangential sections from layer 3 (located between 250 and 350 μm from the pial surface) of the somatosensory cortex (**Figure 3A**).

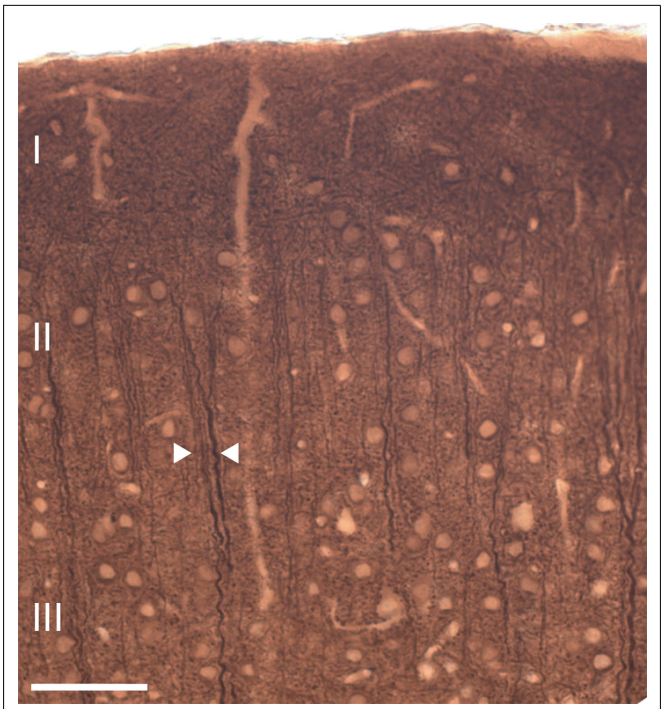

FIGURE 2 | Ascending apical dendrites of cortical pyramidal neurons through several layers of the mouse somatosensory cortex form dendritic bundles. A typical example of a coronal section of the mouse somatosensory cortex showing MAP-2 immunostained dendritic bundles of ascending apical dendrites. Arrows indicate an example of a dendritic bundle. Scale bar 50 μm.

A Voronoi tessellation was performed on the collected dendritic coordinates to analyze the spatial organization of the apical dendrites in wildtype and 5-HT$_{3A}$ receptor knockout mice (**Figure 3B**). The calculated polygon CV indicated that the distribution of apical dendrites in layer 3 of the somatosensory cortex of both wildtype and 5-HT$_{3A}$ receptor knockout mice was clustered (WT; 0.67 ± 0.02, $n = 8$, KO; 0.64 ± 0.02, $n = 5$, n.s.) with no indication that there were differences between the groups.

Subsequently, dendritic bundles were defined using a nearest neighbor distance threshold of 5.5 μm and a minimum number of three dendrites in a bundle (**Figure 3C**). To determine the properties of the spatial distribution of the dendritic bundles, a second Voronoi tessellation was performed on the location coordinates (x_b, y_b) of the above defined bundles (**Figure 3D**).

For wildtype and 5-HT$_{3A}$ receptor knockout mice, the polygon CV was 0.36 ± 0.01 ($n = 8$) and 0.34 ± 0.01 ($n = 5$) respectively, which for both situations is less or equal to 0.36 leading to the conclusion that the dendritic bundles are regularly organized

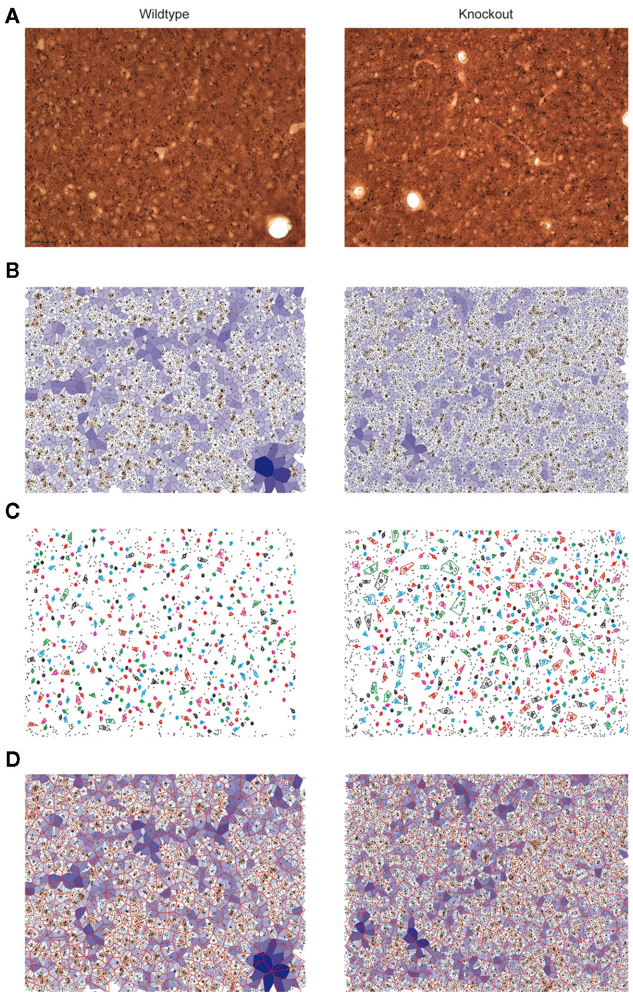

FIGURE 3 | Quantitative analysis of dendritic bundles in the mouse somatosensory cortex of wildtype (left) and 5-HT$_{3A}$ receptor knockout mice (right). Typical examples of **(A)** MAP-2 immunostained tangential sections show clusters of ascending apical dendrites of pyramidal neurons (seen from above as small black circles). **(B)** The polygons obtained using the Voronoi tessellation where the surface associated with each dendrite is indicated with a color scale from small (red) to large (blue). **(C)** Dendritic bundles as defined using a nearest neighbor threshold of 5.5 μm and a minimum of three dendrites in a bundle. Colored circles indicate the center of the bundles, drawn colored polygon indicates the outer circumference of the bundle and thus its size **(D)** Bundle polygons (red honeycomb structure) superimposed on the dendrite polygons. Scale bar 50 μm.

Table 1 | Quantitative analysis of dendritic bundle properties in tangential sections from layer 3 of the somatosensory cortex of wildtype and 5-HT$_{3A}$ receptor knockout mice.

	WT, $N = 8$	KO, $N = 5$
Average diameter dendrites (μm)	1.5 ± 0.01	1.5 ± 0.02
CV dendrites	0.67 ± 0.02	0.64 ± 0.02
Dendritic density (per mm^2)	14232 ± 881	16504 ± 1233
CV dendritic bundles	0.36 ± 0.01	0.34 ± 0.01
Bundle density (per mm^2)	1977 ± 103	1947 ± 76
Average dendritic bundle surface (μm^2)	31 ± 4	56 ± 9*
Average center-to-center distance (μm)	25.3 ± 0.6	25.6 ± 0.5
Number of dendrites per bundle	5.4 ± 0.2	6.7 ± 0.5

Analysis was performed on 0.244 mm^2 tangential sections from layer 3 immunostained for MAP-2 of eight wildtype and five knockout mice (mean ± SEM). CV, coefficient of variation. ∗Indicates a significant difference between wildtype and KO group ($p < 0.05$). Number of dendrites per bundle was tested using a Mann–Whitney test for non-parametric data.

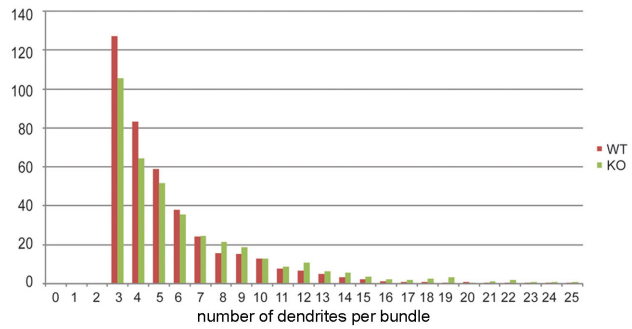

FIGURE 4 | Histogram showing the distribution of the number of dendrites per bundle in tangential sections of the somatosensory cortex of wildtype and 5-HT$_{3A}$ receptor knockout mice.

(Duyckaerts et al., 1994). In addition, dendritic bundles are not differently organized in both groups of animals. Numerical properties of the dendritic bundles defined above for wildtype and 5-HT$_{3A}$ receptor knockout mice are given in **Table 1**.

Within the optical resolution the mean dendritic diameter was the same in both groups. Also the number of dendrites per mm^2, the number of dendritic bundles per mm^2, and mean center-to-center distance between neighboring bundles were not different in wildtype and 5-HT$_{3A}$ receptor knockout mice.

To analyze the distribution of the number of dendrites per bundle a histogram was made (**Figure 4**). Although a tendency toward an increase in the number of dendrites per bundle in 5-HT$_{3A}$ receptor knockout mice was observed, the difference did not reach statistical significance. The analysis of the mean bundle surface of wildtype and 5-HT$_{3A}$ receptor knockout mice, calculated as described in the Section "Materials and Methods" (**Figure 5A**), showed that bundle surface was almost twice as large in 5-HT$_{3A}$ receptor knockout mice than in wildtype mice (WT; 31 ± 4 μm^2, $n = 8$, KO; 57 ± 9 μm^2, $n = 5$, $p < 0.05$, **Figure 5B**).

To investigate the spatial organization of reelin-positive Cajal–Retzius cells, we performed a reelin staining to visualize Cajal–Retzius cells. At P4 and at P14, a similar number of reelin-positive Cajal–Retzius cells could be observed in tangential sections from layer 1 of the somatosensory cortex of wildtype and 5-HT$_{3A}$ receptor knockout mice (**Figures 6A,B**). A typical decrease in the number of reelin-positive Cajal–Retzius cells between P4 and P14 was found in wildtype (46%) as well as in 5-HT$_{3A}$ receptor knockout mice (38%; **Table 2**).

A Voronoi tessellation was performed on the location coordinates of Cajal–Retzius cells and the polygon CV was calculated as described above for dendrites and bundles. Analysis showed that

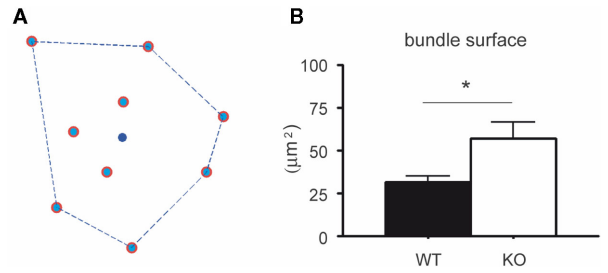

FIGURE 5 | Surface of the dendritic bundles in layer 3 of the somatosensory cortex of wildtype and 5-HT$_{3A}$ receptor knockout mice. **(A)** Bundle surface is determined by the polygon that connects dendrites in the bundle so that its circumference is the smallest one possible, while all dendrites in the bundle are localized within that polygon. The blue dot in the center represents the center of gravity (x_b, y_b). **(B)** The mean surface of layer 3 dendritic bundles in the somatosensory cortex is larger in 5-HT$_{3A}$ receptor knockout mice than in wildtype mice ($p < 0.05$).

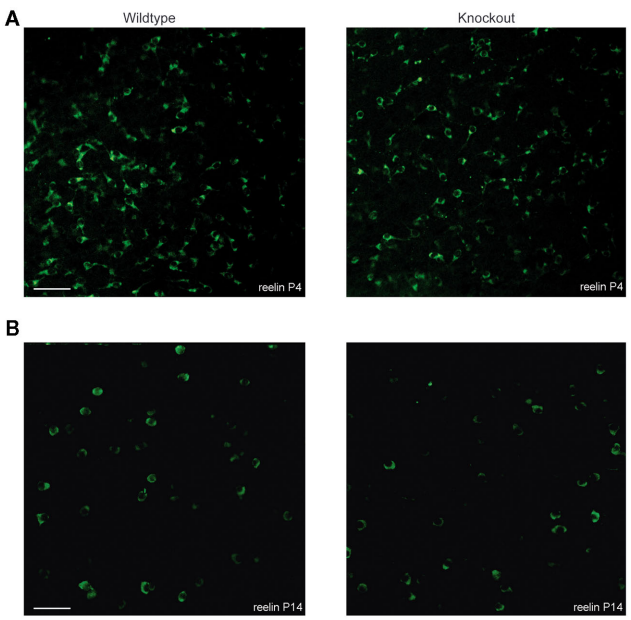

FIGURE 6 | Tangential sections showing the distribution of reelin-positive Cajal–Retzius cells in the somatosensory cortex of both wildtype and 5-HT$_{3A}$ receptor knockout mice. Typical examples of reelin-positive Cajal–Retzius cells in P4 **(A)** and P14 **(B)** tangential sections of the somatosensory cortex of both wildtype and 5-HT$_{3A}$ receptor KO mice. Scale bar 50 µm.

for both P4 and P14 wildtype and 5-HT$_{3A}$ receptor knockout mice, the distribution of reelin-positive Cajal–Retzius cells was random, not clustered, and not different between the two genotypes (**Table 2**).

Table 2 | Quantitative analysis of reelin-positive immunostained Cajal–Retzius cells in tangential sections of 0.21 mm^2 from layer 1 of the somatosensory cortex of wildtype and 5-HT$_{3A}$ receptor KO mice.

	WT, $N = 3$	KO, $N = 4$
Age	**P4**	**P4**
CV Cajal–Retzius cells	0.40 ± 0.01	0.38 ± 0.02
Cajal–Retzius cell density (per mm^2)	598 ± 54	656 ± 7
Age	**P14**	**P14**
CV Cajal–Retzius cells	0.40 ± 0.02	0.35 ± 0.04
Cajal–Retzius cell density (per mm^2)	275 ± 9	251 ± 21

Analysis was performed on reelin layer 1 P4 and P14 tangential sections of three wildtype and four knockout mice. CV, coefficient of variation.

DISCUSSION

In the current study, we quantified the spatial organization of ascending apical dendrites of pyramidal neurons which are organized in dendritic bundles in the somatosensory cortex of both wildtype and 5-HT$_{3A}$ receptor knockout mice. In layer 3 tangential sections of the somatosensory cortex of 5-HT$_{3A}$ receptor knockout mice, the average bundle surface is larger than in wildtype mice. To investigate dendritic bundle organization of both wildtype and 5-HT$_{3A}$ receptor knockout mice we used a similar approach as Vercelli et al. (2004) to show that in both groups the distribution of layer 3 apical dendrites was clustered while the distribution of the dendritic bundles was regular. In concordance with a study of White and Peters (1993), who reported a bundle density of 1918 bundles per mm^2 and an average center-to-center distance between 22 and 25 µm in the mouse somatosensory cortex, here it was shown that dendritic bundles which in the current study consisted of at least three dendrites, have a bundle density of 1978 bundles per mm^2 and mean center-to-center distance of 25 µm in wildtype mice. In line with previous studies, we also observed single dendrites that did not belong to a dendritic bundle. Earlier work from Peters and Kara (1987) and White and Peters (1993) have traced these dendrites and found that these dendrites were either from layer 4 neurons or layer 5 neurons that did not participate in bundles. Since we only analyzed layer 3 of the somatosensory cortex we assume that these single dendrites have the same origin as described earlier.

It has been reported that in the postnatal cortex serotonin is the main excitatory drive for 5-HT$_3$ receptor-expressing Cajal–Retzius cells and that reelin controls dendritic maturation of cortical pyramidal neurons (Chameau et al., 2009). During postnatal development, transient patches of serotonergic innervation have been observed in the rat somatosensory and visual cortex, suggesting a role for serotonin in orchestrating cortical cytoarchitecture (D'Amato et al., 1987; Nakazawa et al., 1992). Interestingly, in neonatal mice of which the serotonergic innervation to layer 1 Cajal–Retzius cells was depleted, reelin levels were decreased and cortical column organization was disrupted (Janusonis et al., 2004). Based on the current observation that dendritic bundle surface is larger in 5-HT$_{3A}$ receptor knockout mice, we suggest a relation between dendritic maturation and dendritic bundle formation in the somatosensory cortex and a role for reelin in regulating these events.

According to the hypothesis of Nishikawa et al. (2002), the distribution of Cajal–Retzius cells determines where dendritic bundles develop by forming reelin-rich cylindrical zones in which

migrating neurons and their dendritic extensions do not settle. By showing a similar number and distribution of Cajal–Retzius cells at P4 and P14 in layer 1 tangential sections of both wildtype and 5-HT_{3A} receptor knockout mice, we ruled out the possibility that the observed differences in dendritic bundle surface were a mere consequence of a change in the number and distribution of reelin-positive Cajal–Retzius cells. Nevertheless, additional studies should be performed at several stages of development and in particular during the first postnatal days when the Cajal–Retzius cell density is the highest, to examine whether a relation between the distribution of Cajal–Retzius cells and the position of dendritic bundles exists or not. In these studies the spatial organization of Cajal–Retzius cells and dendritic bundles needs to be compared and the average distance between Cajal–Retzius cells and dendritic bundles needs to be determined.

It has to be mentioned that also a number of other factors have been implicated to play a role in dendritic bundle formation such as neurotrophins, cell adhesion molecules, gap junctions, and cytoskeletal changes (Ichinohe et al., 2003b; Miyashita et al., 2010). Additionally, it has been proposed that already during early development, sibling cells originating from a single radial glia cell, form the basis of radial columns of interconnected cells (Costa and Hedin-Pereira, 2010). In another study, it was shown that postmitotic pyramidal precursors that migrate into the medial limbic cortex during the first postnatal week, develop dendritic bundles in layer 1 (Zgraggen et al., 2011). Most likely, the formation of dendritic bundles in several areas of the cortex results from a complex interplay between these factors. However, whether one of these other factors has contributed to the changes in dendritic bundle surface in the somatosensory cortex of 5-HT_3 receptor knockout mice remains elusive.

In the cortex, information processing occurs through local cortical microcircuits which show both interlaminar and intralaminar connections (Thomson and Bannister, 2003). It has been suggested that dendritic bundles of ascending apical dendrites of cortical layer 5 pyramidal neurons form the center of cortical modules of vertically interconnected neurons which share functional properties (Peters and Sethares, 1996; Mountcastle, 1997). Labeling studies in both the visual and motor cortex suggested that pyramidal neurons from the same bundle project to the same target, thereby supporting the idea that dendritic bundles are functionally related (Lev and White, 1997; Vercelli et al., 2004; Innocenti and Vercelli, 2010). However, in another study it was shown that synaptic connectivity is independent of apical dendrite bundling (Krieger et al., 2007). Only when vertically aligned pyramidal neurons originate from the same radial glia cell and are thus siblings, they prefer to form synaptic connections (Yu et al., 2009). Although investigation about the functional relevance of dendritic bundles in the cortex is still ongoing, it remains interesting to speculate about the functional consequences of alterations in apical dendrite bundling as observed in the current study in 5-HT_{3A} receptor knockout mice. The fact that in 5-HT_{3A} receptor knockout mice the surface of these bundles is increased, could imply that connectivity between neurons has changed which could lead to alterations in information processing in the cortex of these mice. However, if indeed alterations in information processing in 5-HT_{3A} receptor knockout mice would be observed, they might also be a consequence of the previously observed alterations in dendritic complexity of cortical layer 2/3 pyramidal neurons (Chameau et al., 2009).

In conclusion, the results from the current study show that in the somatosensory cortex of 5-HT_{3A} receptor knockout mice, dendritic bundle size is different from wildtype mice. This finding, together with previously observed differences in dendritic complexity of cortical layer 2/3 pyramidal neurons and cortical reelin levels, suggests an important role for the 5-HT_3 receptor in determining the spatial organization of cortical connectivity in the mouse somatosensory cortex.

ACKNOWLEDGMENTS

We would like to thank Erik Manders from the van Leeuwenhoek Centre for Advanced Microscopy for assistance in making the confocal images, Madhvi Nazir for assistance with the immunohistochemical stainings and David Julius (University of San Francisco, San Fransisco, CA, USA) for providing the 5-HT_{3A} knockout mice.

REFERENCES

Chameau, P., Inta, D., Vitalis, T., Monyer, H., Wadman, W. J., and van Hooft, J. A. (2009). The N-terminal region of reelin regulates postnatal dendritic maturation of cortical pyramidal neurons. *Proc. Natl. Acad. Sci. U.S.A.* 106, 7227–7232.

Costa, M. R., and Hedin-Pereira, C. (2010). Does cell lineage in the developing cerebral cortex contribute to its columnar organization? *Front. Neuroanat.* 4:26. doi:10.3389/fnana.2010.00026

D'Amato, R. J., Blue, M. E., Largent, B. L., Lynch, D. R., Ledbetter, D. J., Molliver, M. E., and Snyder, S. H. (1987). Ontogeny of the serotonergic projection to rat neocortex: transient expression of a dense innervation to primary sensory areas. *Proc. Natl. Acad. Sci. U.S.A.* 84, 4322–4326.

D'Arcangelo, G., Miao, G. G., Chen, S. C., Soares, H. D., Morgan, J. I., and Curran, T. (1995). A protein related to extracellular matrix proteins deleted in the mouse mutant reeler. *Nature* 374, 719–723.

Duyckaerts, C., and Godefroy, G. (2000). Voronoi tessellation to study the numerical density and the spatial distribution of neurons. *J. Chem. Neuroanat.* 20, 83–92.

Duyckaerts, C., Godefroy, G., and Hauw, J. J. (1994). Evaluation of neuronal numerical density by Dirichlet tessellation. *J. Neurosci. Methods* 51, 47–69.

Escobar, M. I., Pimienta, H., Caviness, V. S. Jr, Jacobson, M., Crandall, J. E., and Kosik, K. S. (1986). Architecture of apical dendrites in the murine neocortex: dual apical dendritic systems. *Neuroscience* 4, 975–989.

Fleischhauer, K., Petsche, H., and Witkowski, W. (1972). Vertical bundles of dendrites in the neocortex. *Z. Anat. Entwicklungsgesch.* 136, 213–223.

Ichinohe, N., Fuijyama, F., Kaneko T., and Rockland, K. S. (2003a). Honeycomb-like mosaic at the border of layers 1 and 2 in the cerebral cortex. *J. Neurosci.* 23, 1372–1382.

Ichinohe, N., Yoshihara, Y., Hashikawa, T., and Rockland, K. S. (2003b). Developmental study of dendritic bundles in layer 1 of the rat granular retrosplenial cortex with special reference to cell adhesion molecule, OCAM. *Eur. J. Neurosci.* 18, 1764–1774.

Innocenti, G. M., and Vercelli, A. (2010). Dendritic bundles, minicolumns, columns and cortical output units. *Front. Neuroanat.* 4:11. doi:10.3389/neuro.05.011.2010

Janusonis, S., Gluncic, V., and Rakic, P. (2004).Early serotonergic projections to Cajal-Retzius cells: relevance for cortical development. *J. Neurosci.* 24, 1652–1659.

Krieger, P., Kuner, T., and Sakmann, B. (2007). Synaptic connections between layer 5B pyramidal neurons in mouse somatosensory cortex are independent of apical dendrite bundling. *J. Neurosci.* 27, 11473–11482.

Lev, D. L., and White, E. L. (1997). Organization of pyramidal cell apical dendrites and composition of dendritic clusters in the mouse: emphasis on primary motor cortex. *Eur. J. Neurosci.* 9, 280–290.

Miyashita, T., Wintzer, M., Kurotani, T., Konishi, T., Ichinohe, N., and Rockland, K. S. (2010). Neurotrophin-3 is involved in the formation of apical dendritic bundles in cortical layer 2 of the rat. *Cereb. Cortex* 20, 229–240.

Mountcastle, V. B. (1997). The columnar organization of the neocortex. *Brain* 120, 701–722.

Nakazawa, M., Koh, T., Kani, K., and Maeda, T. (1992). Transient patterns of serotonergic innervation in the rat visual cortex: normal development and effects of neonatal enucleation. *Brain Res. Dev. Brain Res.* 66, 77–90.

Nishikawa, S., Goto, S., Hamasaki, T., Yamada, K., and Ushio, Y. (2002). Involvement of reelin and Cajal-Retzius cells in the developmental formation of vertical columnar structures in the cerebral cortex: evidence from the study of mouse presubicular cortex. *Cereb. Cortex* 12, 1024–1030.

Peters, A., and Kara, D. A. (1987). The neuronal composition of area 17 of rat visual cortex. IV. The organization of pyramidal cells. *J. Comp. Neurol.* 260, 573–590.

Peters, A., and Sethares, C. (1996). Myelinated axons and the pyramidal cell modules in monkey primary visual cortex. *J. Comp. Neurol.* 365, 232–255.

Peters, A., and Walsh, T. M. (1972). A study of the organization of apical dendrites in the somatic sensory cortex of the rat. *J. Comp. Neurol.* 144, 253–268.

Rockland, K. S., and Ichinohe, N. (2004). Some thoughts on cortical minicolumns. *Exp. Brain Res.* 158, 265–277.

Thomson, A. M., and Bannister, A. P. (2003). Interlaminar connections in the cortex. *Cereb. Cortex* 13, 5–14.

Vercelli, A. E., Garbossa, D., Curtetti, R., and Innocenti, G. M. (2004). Somatodendritic minicolumns of output neurons in the rat visual cortex. *Eur. J. Neurosci.* 20, 495–502.

White, E. L., and Peters, A. (1993). Cortical modules in the posteromedial barrel subfield (SM1) of the mouse. *J. Comp. Neurol.* 334, 86–96.

Yu, Y. C., Bultje, R. S., Wang, X., and Shi, S. H. (2009). Specific synapses develop preferentially among sister excitatory neurons in the neocortex. *Nature* 458, 501–504.

Zeitz, K. P., Guy, N., Malmberg, A. B., Dirajlal, S., Martin, W. J., Sun, L., Bonhaus, D. W., Stucky, C. L., Julius, D., and Basbaum, A. I. (2002). The 5-HT3 subtype of serotonin receptor contributes to nociceptive processing via a novel subset of myelinated and unmyelinated nociceptors. *J. Neurosci.* 22, 1010–1019.

Zgraggen, E., Boitard, M., Roman, I., Kanemitsu, M., Potter, G., Salmon, P., Vutskits, L., Dayer, A. G., and Kiss, J. Z. (2011). Early postnatal migration and development of layer II pyramidal neurons in the rodent cingulated/retrosplenial cortex. *Cereb. Cortex.* doi:10.1093/cercor/bhr097. [Epub ahead of print].

Conflict of Interest Statement: The authors declare that the research was conducted in the absence of any commercial or financial relationships that could be construed as a potential conflict of interest.

Received: 30 August 2011; accepted: 12 November 2011; published online: 08 December 2011.

Citation: Smit-Rigter LA, Wadman WJ and van Hooft JA (2011) Alterations in apical dendrite bundling in the somatosensory cortex of 5-HT_{3A} receptor knockout mice. Front. Neuroanat. ***5****:64. doi: 10.3389/fnana.2011.00064*